Fischer, T., Veste, M., Schaaf, W., Dümig, A., Kögel-Knabner, I., Wiehe, W., Bens, O., Hüttl, R. F. (2010): Initial pedogenesis in a topsoil crust 3 years after construction of an artificial catchment in Brandenburg, NE Germany. - Biogeochemistry, 101, 1-3, 165-176

DOI: 10.1007/s10533-010-9464-z

Initial pedogenesis in a topsoil crust three years after construction of an artificial catchment in Brandenburg, NE Germany

Thomas Fischer[1], Maik Veste[2], Wolfgang Schaaf[3], Alexander Dümig[4], Ingrid Kögel-Knabner[4], Wolfgang Wiehe[1], Oliver Bens[5], Reinhard F. Hüttl[3,5]

[1]Brandenburg University of Technology at Cottbus, Faculty of Environmental Sciences and Process Engineering, Central Analytical Laboratory, Konrad-Wachsmann-Allee 6, 03046 Cottbus, Germany

[2]Brandenburg University of Technology at Cottbus, Research Center Landscape Development and Mining Landscapes, Konrad-Wachsmann-Allee 6, 03046 Cottbus, Germany

[3]Brandenburg University of Technology at Cottbus, Faculty of Environmental Sciences and Process Engineering, Chair of Soil Protection and Recultivation, Konrad-Wachsmann-Allee 6, 03046 Cottbus, Germany

[4]Lehrstuhl für Bodenkunde, Department für Ökologie und Ökosystemmanagement, Technische Universität München, D-85350 Freising-Weihenstephan, Germany

[5]GFZ German Research Centre for Geosciences, Telegrafenberg, 14473 Potsdam, Germany

Tel: +49 355 692840

Fax: +49 355 692840

e-mail: thomas.fischer@tu-cottbus.de

Type of contribution: research paper, special issue "BIOGEOMON"

number of text pages: 22

number of tables: 1

number of figures: 9

Abstract

Cyanobacteria and green algae present in biological soil crusts are able to colonize mineral substrates even under extreme environmental conditions. As pioneer organisms, they play a key role during the first phases of habitat colonization. A characteristic crust was sampled three years after installation of the artificial water catchment “Chicken creek”, thus representing an early successional stage of ecosystem development. Mean annual rainfall and temperature were 559 mm and 9.3 °C, respectively. We combined scanning electron microscopy (SEM/EDX) and infrared (FTIR) microscopy to study the contact zone of algal and cyanobacterial mucilage with soil minerals in an undisturbed biological soil crust and in the subjacent sandy substrate. The crust was characterized by an approximately 50 µm thick surface layer, where microorganisms resided and where mineral deposition was trapped, and by an approximately 2.5 mm thick lower crust where mineral particles were stabilized by organo-mineral structures. SEM/EDX microscopy was used to determine the spatial distribution of elements, organic compounds and minerals were identified using FTIR microscopy and x-ray diffraction (XRD). The concentration of organic carbon in the crust was about twice as much as in the parent material. Depletion of Fe, Al and Mn in the lower crust and in the subjacent 5 mm compared to the geological substrate was observed. This could be interpreted as the initial phase of podzolization. Existence of bridging structures between mineral particles of the lower crust, containing phyllosilicates, Fe compounds and organic matter (OM), may indicate the formation of organo-mineral associations. pH decreased from 8.1 in the original substrate to 5.1 on the crust surface three years after construction, pointing to rapid weathering of carbonates. Weathering of silicates could not be detected.

Key words: Biological soil crust, Initial ecosystem, Scanning electron microscopy, FTIR microscopy

Introduction

First colonizers of new land surfaces are cryptogames which often form biological soil crusts (BSC) covering the first millimeter of the top soil in various ecosystems from polar to desert environments. Under Central European conditions they often precede higher vegetation and disappear under conditions of limited light when vegetation or organic soil horizons cover the surface. Hence, they can be considered as an early successional stage in ecosystem development. These BSC are assemblages of cyanobacteria, green algae, mosses, liverworts, fungi and/or lichens (Belnap and Lange, 2001). As pioneer organisms, they play a key role during the first phase of habitat colonization, which is characterized by intense interaction of recently produced organic matter with the geological substrate (Banfield et al., 1999). There is little information on biological soil crusts from the pedogenetic point of view. BSC built up by cyanobacteria and green algae tend to reduce infiltration and generate runoff (Verrecchia et al. 1995, Yair 2001). Factors of soil formation, such as time, climate, vegetation, parent material, relief and human influence predefine soil forming processes. In pedogenesis, time is the factor which determines the degree of accumulation and translocation of weathering and synthesis products in the solum, and it is not likely to expect well developed and distinguished horizons when microbial colonization of parent material starts and prior to the settlement of higher plants.

The aim of this study was to identify initial pedogenesis in situ on a micro-scale level under conditions of incipient interaction with organic matter. A particular crust type, which is common on sandy substrates of the region, served as a model system for pedogenesis under field conditions. To achieve this aim, we combined small-scale bulk chemical analyses with micro-imaging techniques, like SEM-EDX and FTIR microscopy.

Material and Methods

The artificial catchment “Chicken Creek” was constructed in an opencast mine close to Cottbus (about 150 km south east of Berlin, Germany;N 51°36´408, E 14°16´988) to study patterns and processes of initial ecosystem development. The catchment with an area of 6.5 ha is composed of Pleistocene sediments during the Saale-glacial period as a terminal moraine with sandy to loamy-sandy texture overlaying a clay layer. Further details on the technical construction works and initial site conditions are given by Kendzia et al. (2008) and Gerwin et al. (2009). The region is characterized by a temperate climate with a sub-continental character (meanannual rainfall: 559 mm $yr^{-1}$and mean annual temperature 9.3 °C).

During the first years of development (2005 – 2008) increasing areas of soil crust formation were observed within the catchment as an initial process of soil surface stabilization against wind and water erosion. To analyze the structure and composition of these crusts, we selected samples which were characteristic for biological soil crusts dominated by cyanobacteria and green algae on sandy substrates of the region (Fischer et al., 2010).

Three undisturbed field-wet samples were taken in May 2008, three years after installation of the artificial catchment from sector „A“ (Figures 1, 2 and 3) using petri dishes. In the laboratory, these samples were subdivided into crust and subjacent bulk material, the latter not adhering to the crust and having a thickness of about 5 mm.

Figure 1 about here

Figure 2 about here

Figure 3 about here

Total carbon (C_t) content and mineralogical composition of the substrate were determined during

installation of the catchment using dry combustion and x-ray diffraction (XRD), respectively. Carbon determination was repeated in the crust and in the subjacent bulk material, pH was determined using a 1:2.5 water extract.

Samples of the original substrate were taken throughout the catchment in a 20 x 20 m grid right after construction works were completed in September 2005 (Gerwin et al., 2009). Samples from 0 – 30 cm from the four closest grid points were used in this study to characterize the original substrate before crust formation.

Subsamples of the undisturbed crust were dehydrated and embedded in low viscosity epoxy resin. The specimen were cut in transversal direction and polished. Optical micrographs and infrared spectra of the crust surface and the lower part of the crust were recorded in this transversal cuts using FTIR microscopy with polished resin outside the crust serving as control, the background was recorded against gold. Subsequently, the specimen was coated with gold and SEM-EDX micrographs and spectra were recorded accordingly.

Further analysis was based on the results of the micro-imaging and was conducted on the crust surface, the lower part of the crust and on the subjacent material taken to 5 mm depth beneath the crust.

Element concentrations of the crust surface, the lower part of the crust and the subjacent material were determined using x-ray fluorescence spectroscopy (EDXRF, Oxford Instruments X-Supreme). For microscopic FTIR and SEM investigation of the crust surface, the samples of the undisturbed crust were dried in a desiccator at -60 MPa at 20 °C. Top view micrographs were taken and reflectance infrared as well as x-ray fluorescence spectra were recorded using an optical microscope (Thermo Nicolet Centaurus) equipped with an infrared spectrometer (FTIR, Thermo Nicolet 380), as well as a scanning electron microscope (SEM, Zeiss DSM 962) equipped with a back scattered electron detector (BSE) and with an energy dispersive x-ray fluorescence

spectrometer after coating with gold (EDX, Oxford Instruments ISIS), respectively. To eliminate the influence of the dominating quartz and to account for the penetration of mid-IR into the sample, quartz was used as background and Kubelka-Munk correction was performed for the FTIR measurements. Spectral correlations were estimated using the Mattson Win1st FTIR software.

Results

The parent material used for construction are Pleistocene sediments taken from the fore-field of the mine where it was deposited during the Saale-glacial period as a terminal moraine (Table 1). The silt and clay contents of the siliceous sandy substrate were 4.3% and 3.0%, respectively. The average content of organic carbon in the crust was 0.53% compared to 0.21% in the bulk material of the subjacent layer. The parent substrate contained 0.28% C_{org} during installation. Organic carbon accumulated predominantly in the crust, where photoautotrophic organisms reside. Though the original substrate contained 0.63% carbonates, it was not detected in the crust, nor in the subjacent material. pH_{H2O} values amounted to 5.1 in the crust and to 5.6 in the subjacent material compared to 8.1 in the parent substrate. SEM-EDX revealed that Ca found in the crust and in the subjacent material was present in feldspars only.

A top view of the crust under the optical microscope and SEM is shown in Figure 4. The surface of the crust is characterized by dense growth of filamentous green algae and of filamentous cyanobacteria, enveloped in sheaths („F“ in Fig. 4) and sticking to the surface of sand grains.

Figure 4 about here

In order to characterize solely the *organic matter* on the surface of the crust (i.e. „PS“ in Fig. 4), FTIR spectra of a spot sized 50 μm x 50 μm and focused on organic material were recorded in situ

using FTIR microscopy. Comparison of the fingerprint region of the sample spectra with reference samples revealed highest correlation of crust organic matter with dextran from Leuconostoc (r=0.75) and with cellulose (r=0.65), but little correlation with Aldrich humic acid Na salt (r=0.07, Fig. 5).

Figure 5 about here

For characterization of *organo-mineral structures* on the surface of the crust, a FTIR spectrum was recorded on a 600 μm x 400 μm spot, which covered an area where both crust organic matter and minerals were present. This spectrum was characterized by organic and siliceous bands (Figure 6). A typical triplet of signals at 3696 cm^{-1}, 3652 cm^{-1} and 3621 cm^{-1} indicated the presence of kaolinite, which may be formed by weathering of K- and Na-feldspars or mica (van der Marel and Beutelspacher, 1976, Wilson, 2004). This finding was confirmed by XRD measurements of the parent material, where mineral analysis of the clay fraction revealed kaolinite and vermiculite concentrations of 9–16% and 3–4%, respectively (Gerwin et al., 2009). Obviously, the kaolinite found on the crust surface was formed in the substrate prior to construction of the catchment or trapped by the crust from atmospheric deposition. The kaolinite bands at 3621 cm^{-1} and 3652 cm^{-1} may interfere with muscovite, which was identified in the sample by SEM-EDX, or with other phyllosilicates, predominantly illite (41–60%) and mixed layer illite/smectite (12–38%; <50% illite), which were identified in the parent material using XRD (Gerwin et al., 2009). Due to the background quartz the signals for Si-O vibrations at approx. 1110 cm^{-1} and 1030 cm^{-1}, which are characteristic for all silicates, seem somewhat suppressed compared to the inner surface Al-OH vibrations of phyllosilicates.

In both surface FTIR spectra, crust organic matter is characterized by -CH bands at 2800-3000 cm^{-1} and by C-O bands at 1050-1300 cm^{-1}, although the latter may interfere with the Si-O bands of silicates. A broad signal at 1500-1800 cm^{-1} may originate from organic -OH, -C=O and -C=C-

vibrations, which may not be assigned unambiguously, or from atmospheric moisture captured during handling of the sample. It is not likely that amides contribute significantly to the spectrum, because their typical signal at 3250-3350 cm^{-1} is missing. Aromatic signals or aliphatic C=C double bindings in the band from 3000 cm^{-1} to approximately 3100 cm^{-1} (=CH) could not be detected in the crust. Therefore, the organic signals of the spectrum point to typical bonds of polysaccharides. There is no clear indication of the presence of humic substances here.

Figure 6 about here

SEM-EDX measurements were conducted at three spots of the transversal cut through the sample, one of them located on the surface of the crust (“S” in Fig. 7), and the other two located approximately 1 mm beneath the surface (”L” in Fig. 7).

Table 1 about here

Figure 7 about here

At the crust surface, which was covered with microbial extracellular polymers (cf. Fig. 5), an approximately 50 µm thick layer of small sized particles was observed („S“ in Fig. 7). In this layer Si was depleted compared to the lower part of the crust and to the subjacent parent material, whereas Al, K, Fe, Ti, Ca, Mn and Sr were accumulated here (Tab. 1).

In the lower part of the crust, these dense formations containing a small sized particle fraction found on the surface could not be observed. In contrast, this layer was more Si rich compared to the crust surface and to the subjacent material. In addition, numerous bridge-like structures were discovered in the contact zone of the parent sand grains, containing Si, Al and small amounts of Fe (Fig. 8). Comparison of FTIR spectra of the bridge-like structure with epoxy resin revealed bands which are typical for both organic matter and phyllosilicates (Fig. 8b). The embedding resin is

characterized by the presence of –CH, Ester-C=O and –OH. Hence, these bands should be disregarded for the interpretation of the sample spectrum. The bridge-like structure contains a characteristic band at 1620-1680 cm^{-1} which cannot be assigned to OH or amide unambiguously. Unlike the surface, the lower part of the crust is characterized by a FTIR band at 1500-1600 cm^{-1} which, in conjunction with the bands at 3000-3100 cm^{-1} (=CH) and at 3250-3350 cm^{-1} (NH), points to C=C double bindings or amides. Matrix interferences caused by the embedding polymer and by silicates are too strong to reasonably correlate this spectrum with humic reference material. In addition, weak signals which are characteristic for inner surface Al-OH vibrations of phyllosilicates at 3620 cm^{-1} and at 3696 cm^{-1} were detected here.

Fe traces observed in the bridge-like structures in the lower part of the crust most likely originate from poorly crystalline (0.05% Fe_o) and crystalline (0.27% Fe_d-Fe_o) iron oxides in the parent material, where the total amount of Fe was 0.86±0.30% (Gerwin et al., 2009). EDX analysis of a single mica flake revealed an Al:Si:K ratio of approximately 3:3:1, pointing to muscovite with small amounts of Fe (Fig. 9), which also may contribute due to the release of Fe by weathering.

Figure 8 about here

Figure 9 about here

Discussion

Accumulation of organic matter in BSC occurs due to photoautotrophic organisms like green algae and cyanobacteria (Belnap and Lange, 2001). There is no indication that crust organisms tended to migrate into depth (Brock, 1975). For biological soil crusts on Dutch inland dunes, Pluis (1994) reported organic matter concentrations ranging from 0.28% OM in young algal crust to 0.43% OM in mature algal crusts, with a background of 0.10% OM in bare drifting sand. After subtraction of the background of OM, the concentration of organic carbon in the crust of this study (0.32%) is

comparable to those of the mature algal crusts as described by Pluis (1994). However, it represents an early stage of crust development three years after installation of the artificial catchment. This is also reflected by organic carbon concentrations ranging from 0.19% to 0.74% C_{org} (background of 0.06% C_{org}) in BSCs on inland dunes located close to the study site (Fischer et al., 2010).

The ability of microorganisms to standardize mineral surfaces to their needs by “active support preconditioning” (Bos et al., 1999; Dufrene et al., 1996) seems to promote mineral-organic associations through the deposition of extracellular polysaccharides and proteins as adhesives. The formation of these “conditioning films’’ moderates eventual differences in the surface chemistry of the underlying substrate and can thus be seen as an adaptation mechanism that allows microorganisms to colonize highly variable types of mineral surfaces (Kögel-Knabner et al., 2008). It has been demonstrated that extracellular polymeric substances (EPS) play a key role in aggregation and for the hydrological properties of soil crusts (Kidron et al., 1999, Fischer et al., 2010). Subsequent microbial utilization of primary organic matter produced by microorganisms may result in microbial neosynthesis of humic substances and in mineralization. Three types of functional surface sites on minerals can be distinguished, which offer different bonding possibilities and strengths to the organic matter (OM): (1) Surfaces inhabited by single coordinated hydroxyl groups are common to Fe and Al oxides, allophane, and imogolite and the edges of layer silicates; (2) siloxane surfaces with permanent layer charge due to isomorphic substitution appear at some 1:2–layer-type phyllosilicates, such as vermiculite, illite, and smectite; (3) siloxane surfaces without layer charge occur in both 1:2–layer-type (talc, pyrophyllite) and in 1:1-type minerals (kaolinite group). Generally, strong protection of OM is correlated with the presence of hydroxylated mineral phases in acidic soil (Kögel-Knabner et al., 2008). To a minor degree, all three above mentioned types of surface sites were present in the BSC due to the composition of the geological substrate (clay fraction with Fe oxides, kaolinite and 1:2–layer-type phyllosilicates) and as a result of deposition (accumulation of fine particles). This may offer the formation of organo-mineral interactions with OM produced by microorganisms, and thus the stabilization of BSC derived

polysaccharides – which were clearly indicated by FTIR spectra – against decomposition. Lignin as a structural component of higher plants is not produced by crust microorganisms (Sarkanen and Ludwig, 1971). Due to the absence of precursors for polycondensed compounds, the small amounts of organic matter containing C=C double bindings in the lower part of the crust most likely presents organic carbon inherited from the parent material (C_{org} concentration of 0.28%) which was used for construction of the catchment.

The accumulation of Al, K Fe Ti, Mn and Sr in the surface 50 µm – layer of the crust (cf. Tab. 1 and Fig. 7) might be explained by colluvial processes, by particulate atmospheric deposition of fine grained material (depositional crust), or by crust formation through raindrop impact (structural crust). For a loess soil, Chen et al. (1980) described three stages during structural crust formation: (1) the initial stage, at which the soil exhibited uniform distribution of the particles; (2) a middle term stage, at which coarse particles, stripped off the fine ones, constituted the surface layer of the soil; and (3) a final stage at which the coarse particles were washed away and a seal skin, about 100 µm thick, is formed at the soil surface. A depositional crust was also characterized by a thin skin about 100 µm thick. The crust investigated in this study did not have a pronounced skin of fine particles, but was characterized by accumulation of fine particles and organic matter in the pores of a sandy matrix (“M” and “PS” in Figure 4), which formed a 50 µm thick surface layer (“S” in Figure 7). Possibly, the amounts of silt and clay in the substrate and deposition of fine particles were too small to undergo the process described by Chen et al. (1980), where silt and clay contents amounted to 7.5% and 15.0%, respectively. It is therefore not possible to assign the crust investigated in this study to one of the stages described by Chen et al. (1980). The accumulation of elements on the crust surface could be caused by atmospheric deposition (Verrecchia et al., 1995, Kidron et al., 2009), because neighboring open-cast lignite mining produces large amounts of dust. However, particles containing high amounts of carbon were not detected. Another possible reason for relative accumulation of Al, K, Fe and other elements in the surface layer of the crust is enhanced dissolution of quartz, which is more susceptible to weathering than muscovite or clay minerals under soil conditions (Jackson et al., 1948).

Weathering of silicates may result in formation of silicic acid from quartz, in formation of aluminium hydroxide, halloysite and kaolinite from K-feldspar and of multi-component weathering products from mica (Wilson, 2004). Interaction of feldspars with organic acids from roots, fungal hyphae or lichens was reported to enhance weathering rates and may result in formation of crystalline Ca oxalate, siliceous relics, aluminous silicate gel-like material and poorly ordered Fe oxide minerals (Jones et al., 1980, Jones et al., 1981). In contrast, Barker and Banfield (1996) investigated the weathering of amphibole syenite by the crust lichens *Rhizocarpon grande*and *Porpidea albocaerulescens*and could find no evidence of ‘‘pervasive leaching’’ of feldspars or other minerals, all of which remained perfectly intact in the lichen thallus, or of the existence of siliceous relics such as were identified by Wilson et al. (1981). They attributed biologically mediated weathering to extracellular organic polymers, most likely acidic mucopolysaccharides, and argued against the role of lichen and oxalic acid as important weathering agents. In fact, not all lichen organisms are able to excrete metal-complexing organic acids and sometimes lichens may actually reduce weathering rates (Wilson, 2004). In the case of mica, the vermiculitization reaction involves exchange of the interlayer K of the mica with ions of the external solution, but may be bypassed under more intensive weathering conditions and conversion of biotite directly to kaolinite may occur (De Kimpe and Tardy, 1968). Biological weathering of mica may occur as a result of uptake by plants of interlayer K and of organic acids excreted by plants or microorganisms (Wilson, 2004).

However, the contribution of mineral weathering to the observed element accumulation within three is expected to be rather small due to low reaction rates. Most likely, small sized particles found at the surface of the crust may be trapped and protected against erosion by the bodies and by exopolysaccharides of crust organisms (Belnap et al., 2000, Belnap and Gillette, 1998). Furthermore, the secretion of exopolysaccharides is stimulated by Mg, K, and Ca, which influence the metal-ion concentration and binding capacity within in the crust (Greene and Darnal, 1999, Belnap et al., 2001).

Weathering of carbonates resulted in a pH decrease from 8.1 in the original substrate to 5.1 in the crust and to 5.6 in the subjacent layer. It has been reported that pH may increase or decrease substantially in the first millimeters of BSCs due to CO_2 uptake or production in sandy soils when the buffering capacity is low (Garcia-Pichel and Belnap, 2001). On the other hand, possible exudation of organic acids by fungal hyphae and other microorganisms (Jones et al., 1980, Jones et al., 1981) may contribute to acidification. Many BSCs have been investigated in arid regions where carbonates are widespread and pH of soils is regulated by the carbonate buffering system, which is active at pH values >6.2. The carbonates, which were initially present in the geological substrate, were leached completely from the crust and silicates dominate regulation of soil pH in the range between 5.0 and 6.2 (Ulrich, 1983; Hüttl and Fischer, 2001). Hence, carbonate leaching, composition of the microbial community, consisting of photoautotrophic proton consumers and heterotrophic proton producers, as well as a soil buffering system that resists pH changes in the range between 5.0 and 6.2 may explain the significant drop of pH in the crust investigated in this study. Spröte et al. (2009) reported pH values in cyanobacterial crusts on an inland dune in NE Germany ranging from 4.9 to 5.2. We assume that the pH of crusts is regulated by the crust microbial community, where it is typically adjusted to values between 4.9 and 5.2 in the cyanobacterial crusts commonly found on quaternary sands in NE Germany.

Podzolization involves translocation of organic substances as well as Fe and Al compounds into depth under conditions of low pH. In various studies from the North-American cold deserts it could be observed that biological soil crusts enhance the content of macro- and micro-nutrients (including N, K, Ca, Fe, Mn, Cl, S, P), that they change the pH-values and element concentrations in the upper first millimeters and that they influence the nutrient uptake by higher plants (Harper and Pendleton, 1993, Harper and Belnap, 2001). The accumulation of fine-grained material plays an important role in the binding of positively charged elements. Nitrogen is accumulated in the soil crusts due to the biological nitrogen fixation (e.g. Rogers and Burns, 1994, Russow et al., 2004). In particular Fe, Al and Mn, were depleted in the lower crust and in the subjacent layer compared to original substrate, which points to leaching of these elements and a relative accumulation of

silicates (Table 1). However, an illuvial horizon, where organic matter, Fe, Al and Mn precipitate, could not be detected. Beside the low available OM content, this could also be due to lateral transport by surface runoff and erosion that frequently occurred in this early poorly vegetated phase of development.

Conclusions

Crust-born accumulation of organic matter was observed only three years after construction of an artificial mineral solum under conditions of temperate climate. Carbonates, present in the original substrate, were completely leached and pH values decreased from 8.1 to 5.1 in the crust within three years. Weathering of silicates could not be detected. These changes in the top mm of the soil surface indicate rapid pedogenic processes induced by the formation of biological soil crusts and possibly by lateral transport with surface runoff that is also promoted by crust formation. The observed changes in topsoil properties could be interpreted as a formation of an initial E horizon at small scale. More investigations are needed to understand the role of biological soil crusts on initial pedogenesis as well as on their temporal and spatial distribution.

Acknowledgments

This study is part of the Transregional Collaborative Research Centre 38 (SFB/TRR 38) which is financially supported by the Deutsche Forschungsgemeinschaft (DFG, Bonn) and the Brandenburg Ministry of Science, Research and Culture (MWFK, Potsdam). The authors thank Vattenfall Europe Mining AG for providing the research site. We also thank Werner Gerwin (BTU Cottbus, Research Center Landscape Development and Mining Landscapes) for providing the location map, Philipp Lange (BTU Cottbus, Research Center Landscape Development and Mining Landscapes) for technical assistance during the measurements and for the kind review of the manuscript, Roland Spröte and Claudia Zimmermann (BTU Cottbus, Chair of Soil Protection and Recultivation) for assistance during sampling. We are grateful to the anonymous reviewers for the truly helpful

comments.

Literature

Banfield JF, Barker WW, Welch SA, Taunton A (1999) Biological impact on mineral dissolution: Application of the lichen model to understanding mineral weathering in the rhizosphere. Proceedings of the National Academy of Sciences of the United States of America 96(7):3404-3411

Barker WW, Banfield JF (1996) Biologically versus inorganically mediated weathering reactions; relationships between minerals and extracellular microbialpolymers in lithobiontic communities. Chemical Geology 132:55-69

Belnap J, Gillette DA (1998) Vulnerability of desert biological soil crusts to wind erosion: the influences of crust development, soil texture, and disturbance. Journal of Arid Environments 39(2):133-142

Belnap J, Lange OL (eds.) (2001) Biological soil crusts: structure, function and management. Ecol. Studies 150, Springer Publisher, Heidelberg-Berlin-New York, 503 pp.

Belnap J, Prasse R, Harper KT (2001) Influence of biologcial soil crusts on aoil environments and vascular plants. In: Belnap J, Lange OL (eds.) Biological soil crusts: structure, fuction and management, Ecologcial Studies 150. Springer, Heidelberg, pp. 281-300

Belnap J, Reynolds R, Reheis M, Phillips SL, (2000) What makes the desert bloom? Contribution of dust and crusts to soil fertility on the Colorado plateau. Shrubland Ecosystem Genetics and Biodiversity: Proceedings. USDA Forest Service Rocky Maintain Research Station Proceedings, volume 21, 147-153

Bos R, van der Mei HC, Busscher HJ (1999) Physico-chemistry of initial microbial adhesive

interactions–its mechanisms and methods for study. FEMS Microbiol. Rev. 23:179-229

Brock TD (1975) Effect of water potential on a Microcoleus (Cyanophyceae) from a desert crust Journal of Phycology 11(3):316-320

Chen Y, Tarchitzky J, Brouwer J, Morin J, Banin A (1980) Scanning electron microscope observations on soil crusts and their formation Soil Science 130(1):49-55

De Kimpe C, Tardy Y (1968) Etude de l'altération d'une biotite en kaolinite par spectroscopie infrarouge. Bulletin de Groupe français des Argiles 19:81-85

Dufrene YF, Boonaert CJP, Rouxhet PG (1996) Adhesion of Azospirillum brasilense: role of proteins at the cell-support interface. Coll. Surfaces B: Biointerfaces 7:113-128

Fischer T, Veste M, Wiehe W, Lange P (2010) Water repellency and pore clogging at early successional stages of microbiotic crusts on inland dunes, Brandenburg, NE Germany. Catena 80:47-52

Garcia-Pichel F, Belnap J, (2001) Small-scale environments and distribution of biological soil crusts. In: Belnap J, Lange OL (eds.) Biological soil crusts: structure, function and management. Springer, Heidelberg, pp. 193-202

Gerwin W, Schaaf W, Biemelt D, Fischer A, Winter S and Hüttl R F (2009) The artificial catchment "Chicken Creek" (Lusatia, Germany) - a landscape laboratory for interdisciplinary studies of initial ecosystem development. Ecol Eng 35(12):1786-1796

Greene B, Darnal DW (1999) Microbial oxygenic photoautotrophs (cyanobaceria and algae) for metal-ion binding.. In: Ehrlich HI, Brierly CI (eds.) Micriobial mineral recovery. Mc Graw-Hill, New

York, pp. 277-302

Harper KT Pendleton RL (1993) Cyanobacteria and cyano-lichens: can they enhance availability of essential minerals for higher plants? Great Basin Nat 53:59-72

Harper KT, Belnap J (2001) The influence of biologcial soil crusts on minieral uptake by associated seed plants. J Arid Environ 47:347-357

Hüttl RF, Fischer T (2001) Wirkungen auf den Boden. In: Guderian R (ed.) Handbuch der Umweltveränderungen und Ökotoxikologie, Band 2A: Terrestrische Ökosysteme. Springer, Berlin, Heidelberg, New York, pp. 31-90

Jackson ML, Tyler SA, Willis AL, Bourbaeu GA, Pennington RP (1948) Weathering sequence of clay size minerals in soils and sediments. 1. Fundamental generalizations Journal of Physical and Colloid Chemistry 52(7):1237-1260

Jones D, Wilson MJ, McHardy WJ (1981) Lichen weathering of rock-forming minerals: application of scanning electron microscopy and microprobe analysis. Journal of Microscopy 124:95-104

Jones D, Wilson MJ, Tait JM (1980) Weathering of a basalt by Pertusaria corallina. The Lichenologist 12:277-289

Kendzia G, Reißmann R, Neumann T (2008) Targeted development of wetland habitats for nature conservation fed by natural inflow in the post-mining landscape of Lusatia. World of Mining 60:88-95

Kidron GJ, Yaalon DH, Vonshak A (1999) Two causes for runoff initiation on microbiotic crusts: Hydrophobicity and pore clogging. Soil Science 164(1):18-27

Kidron GJ, Vonshak A, Abeliovich A (2009) Microbiotic crusts as biomarkers for surface stability and wetness duration in the Negev Desert. Earth Surf. Process. Landforms 34:1594-1604

Kögel-Knabner I, Guggenberger G, Kleber M, Kandeler E, Kalbitz K, Scheu S, Eusterhues K, Leinweber P (2008) Organo-mineral associations in temperate soils: Integrating biology, mineralogy, and organic matter chemistry. J Plant Nutr Soil Sci 171:61-82

Pluis JLA (1994) Algal crust formation in the inland dune area, Laarder Wasmeer, the Netherlands Vegetatio 113(1):41-51

Rogers SL, Burns RG (1994) Changes in aggregate stability, nutrient status, indegenous microbial populations, and seedling emergernce, following inocaltion of soil with Nostoc muscorum. Biol Fertil Soils 18:209-215

Russow R, Veste M, Littmann T (2004) Using the natural 15N-abundance to assess the major nitrogen inputs into the sand dune area of the north-western Negev Desert (Israel). Isotopes in Environmental and Health Studies 40:57-67

Sarkanen KV, Ludwig CH, eds. (1971) Lignins: Occurrence, Formation, Structure and Reactions. Wiley-Inter- science. New York.

Spröte R, Veste M, Fischer T, Lange P, Bens O, Raab T, Hüttl RF (2009) Development of biologicalsoil crusts in initial ecosystems in Lusatia, Germany. In: DBG Jahrestagung 2009 Bonn "Böden - eine endliche Ressource", 05.-13.09.2009, Bonn

Ulrich B (1983) Soil acidity and its relations to acid deposition. In: Ulrich B, Pankrath J (eds.) Effects of accumulation of air pollutants in forest ecosystems. Reidel, Boston, pp. 127-146

van der Marel HW, Beutelspacher H (1976) Atlas of infrared spectroscopy of clay minerals and their admixtures. Elsevier, 396 pp.

Verrecchia E, Yair A, Kidron GJ, Verrecchia K. 1995. Physical properties of the psammophile cryptogamic crust and their consequences to the water regime of sandy softs, north-western Negev Desert, Israel. Journal of Arid Environments 29: 427-437.

Wilson MJ (2004) Weathering of the primary rock-forming minerals: processes, products and rates. Clay Minerals 39:233-266

Wilson MJ, Jones D, McHardy WJ (1981) The weathering of serpentinite by Lecanora atra. The Lichenologist 13:167-176

Yair, A. 2001. Soil crusts and water redistribution in Israel. Belnap J, Lange OL, editors. Biological soil crusts. structure, function and management. Ecological Studies 150, Springer Publisher, Heidelberg-Berlin-New York. p304-314.

Figures

Figure 1 Location map of the artificial water catchment „Chicken Creek“, backslope with sectors A – D (1), footslope (2) and lake basin (3), sampling point

Figure 2 General photograph of the study site

Figure 3 Photograph of the crust during sampling.

Figure 4 Top view of the BSC under optical microscope (a) and under SEM (b), F – microbial filament, PS – polymeric substance sticking to the surface of a sand particle, M – mineral debris trapped on the surface of the crust.

Figure 5 Fingerprint region of the FTIR spectra of crust organic matter recorded on a 50 x 50 μm^2 spot, dextran from Leuconostoc (Aldrich), microcristalline cellulose (Spex CertiPrep), humic acid Na salt (Aldrich) and quartz. Crust organic matter was recorded using quartz as background, Kubelka-Munk correction was applied. Structural differences appear more pronounced in the fingerprint region, because >1800 cm^{-1}all organic substances were characterized by similar -CH and -OH vibrations. Background quartz is displayed for reference.

Figure 6 FTIR spectrum of a larger spot of the crust surface (600 x 400 μm^2) both organic matter and minerals were present, including band assignments (bold solid lines). Crust surface was recorded using quartz as background, Kubelka-Munk correction was applied.

Figure 7 Transversal cut of the BSC, embedded in low viscosity epoxy resin. Overview SEM micrograph (left) and Si, Al and K mapping of the surface (right). Feldspars appear brighter than quartz due to higher K and Ca contents. “S“ is the ~50 µm thick surface layer where small sized

mineral particles accumulated, “L” is the lower crust.

Figure 8 Transversal cut of the BSC, embedded in low viscosity epoxy resin. (a) Overview SEM micrograph (left) and Si, Al and Fe mapping of an organo-mineral bridge between quartz particles (right). (b) FTIR spectra of the embedding epoxy resin, taken outside of the crust (I) and the organo-mineral bridge-like structure (II)

Figure 9 Transversal cut (a) and EDX spectrum (b) of mica from the BSC studied. The spectrum was recorded at spot 1. The Si:Al:K intensity ratio is approximately 3:3:1, which points to muscovite ($KAl_2(AlSi_3O_{10})(F,OH)_2$). The oxygen signal is suppressed due to low detector sensitivity at <1 keV.

Table 1 Element concentrations (mean values, m and standard deviations, s) of the crust surface, the lower part of the crust (n=3), the subjacent material and the original substrate used for construction (n = 4), determined with EDXRF, C_{org} concentrations, determined by dry combustion, and pH_{H2O} (1:2.5) (n=3)

	crust surface (0-0.05 mm)		lower crust (0.05-2.5 mm)		subjacent (2.5-7.5 mm)		original substrate (0-30 cm)	
	m	s	m	s	m	s	m	s
% Si	41.39	0.04	43.69	0.18	43.54	1.35	38.58	1.31
% Al	1.69	0.08	1.19	0.04	1.31	0.07	5.01	0.26
% K	1.13	0.04	0.91	0.12	0.87	0.40	0.92	0.47
% Fe	0.72	0.02	0.29	0.01	0.28	0.05	1.69	0.31
% Ti	0.38	0.01	0.11	0.03	0.11	0.02	0.38	0.10
% Ca	0.16	0.01	0.12	0.01	0.12	0.07	1.60	0.88
% C_{org} [1)]	0.53	0.11			0.21	0.04	0.28	0.20
mg Mn kg^{-1}	133	10	70	2	69	12	380	81
mg Sr kg^{-1}	164	7	127	28	98	21	91	20
pH [1)]	5.1	0.2			5.6	0.1	8.1	0.1

[1)] C_{org} and pH were determined for the entire crust (0-2.5 mm)

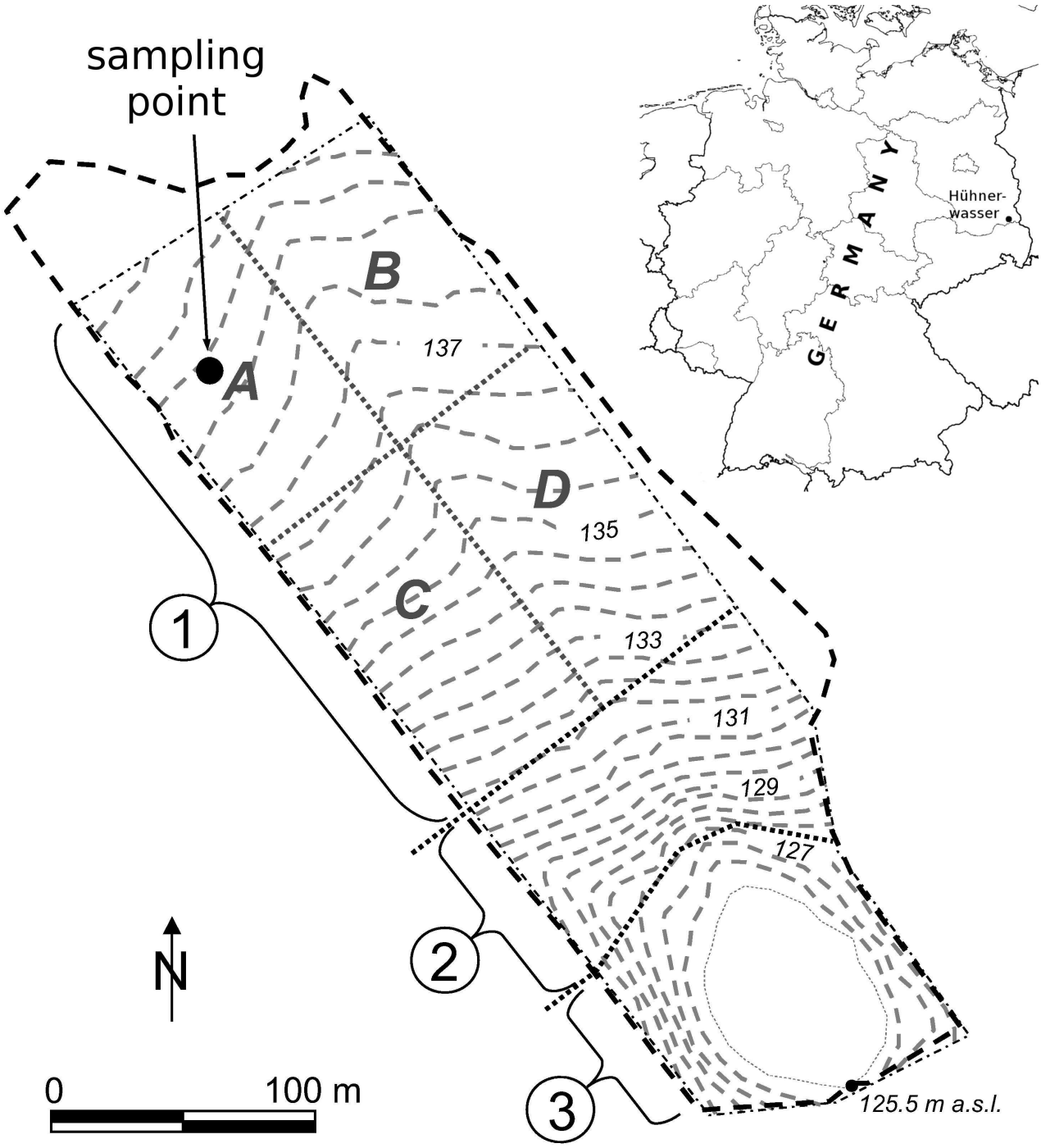
sampling
point
A
B
C
D
137
135
133
131
129
127
1
2
3
N
0
100 m
125.5 m a.s.l.
GERMANY
Hühner-
wasser

Figure 1

Figure 2

Figure 3

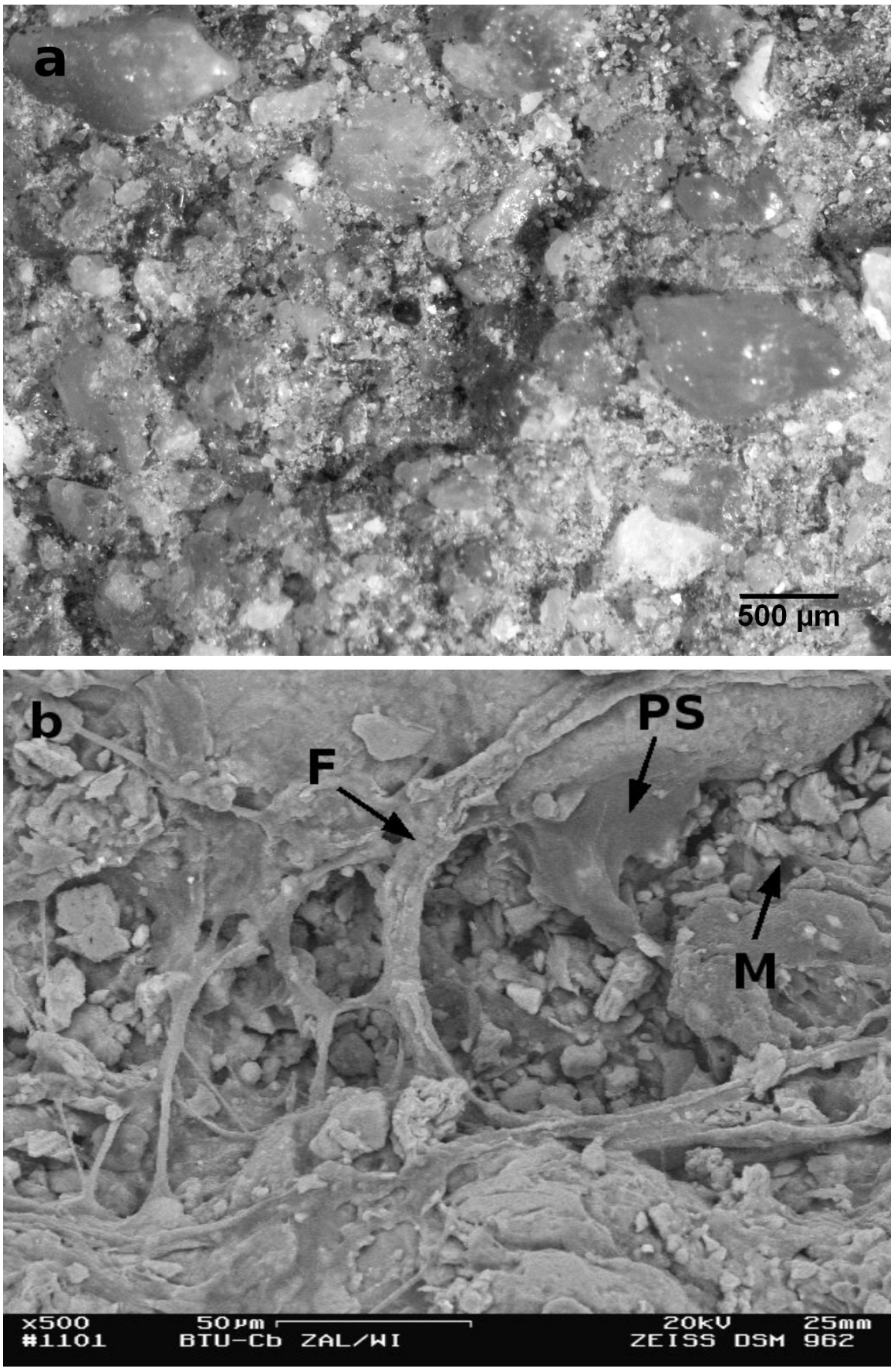
a
500 µm
b
PS
F
M
x500
#1101
50µm
BTU-Cb ZAL/WI
20kV
25mm
ZEISS DSM 962

Figure 4

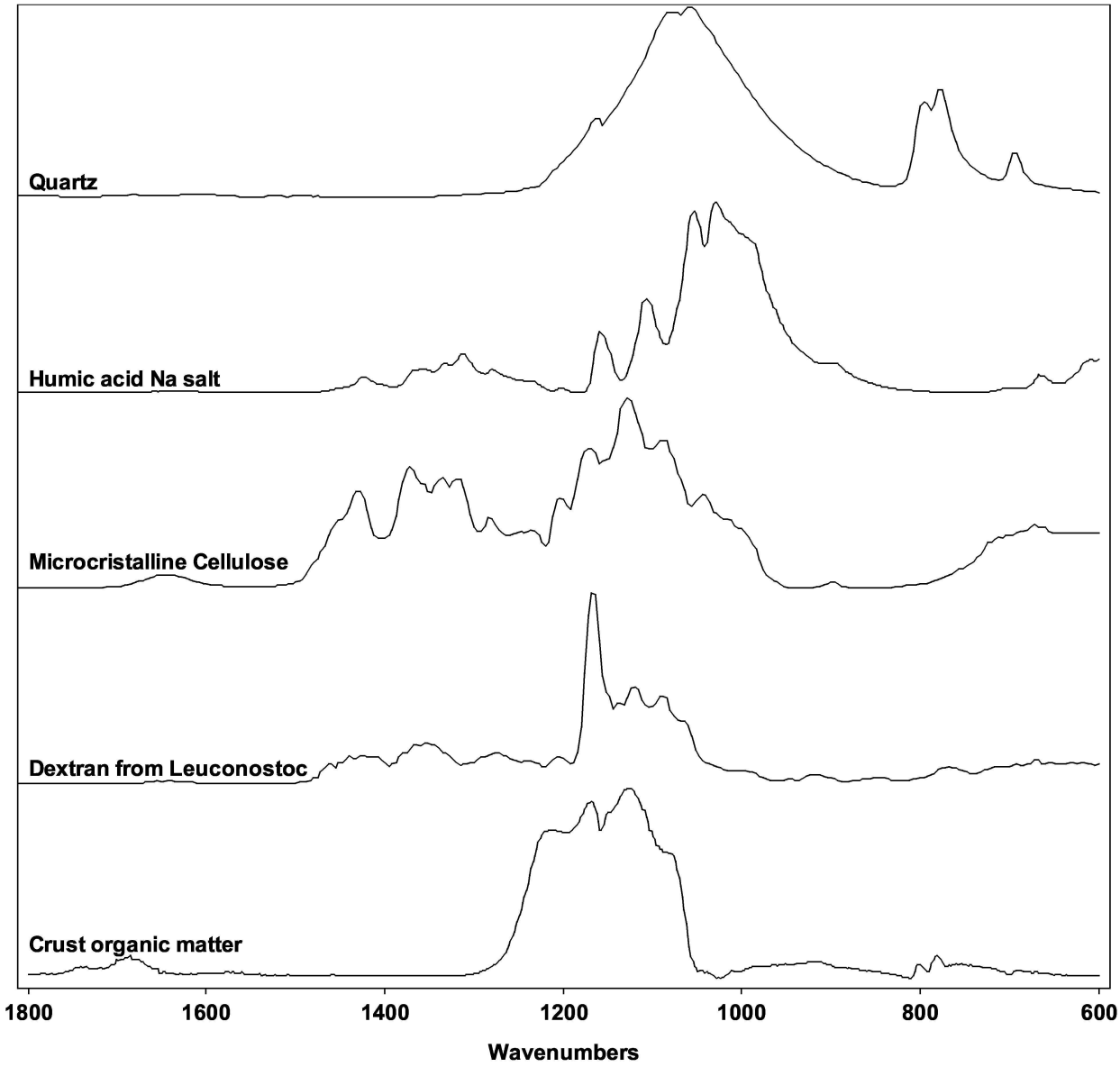
Quartz
Humic acid Na salt
Microcristalline Cellulose
Dextran from Leuconostoc
Crust organic matter
1800
1600
1400
1200
1000
800
600
Wavenumbers

Figure 5

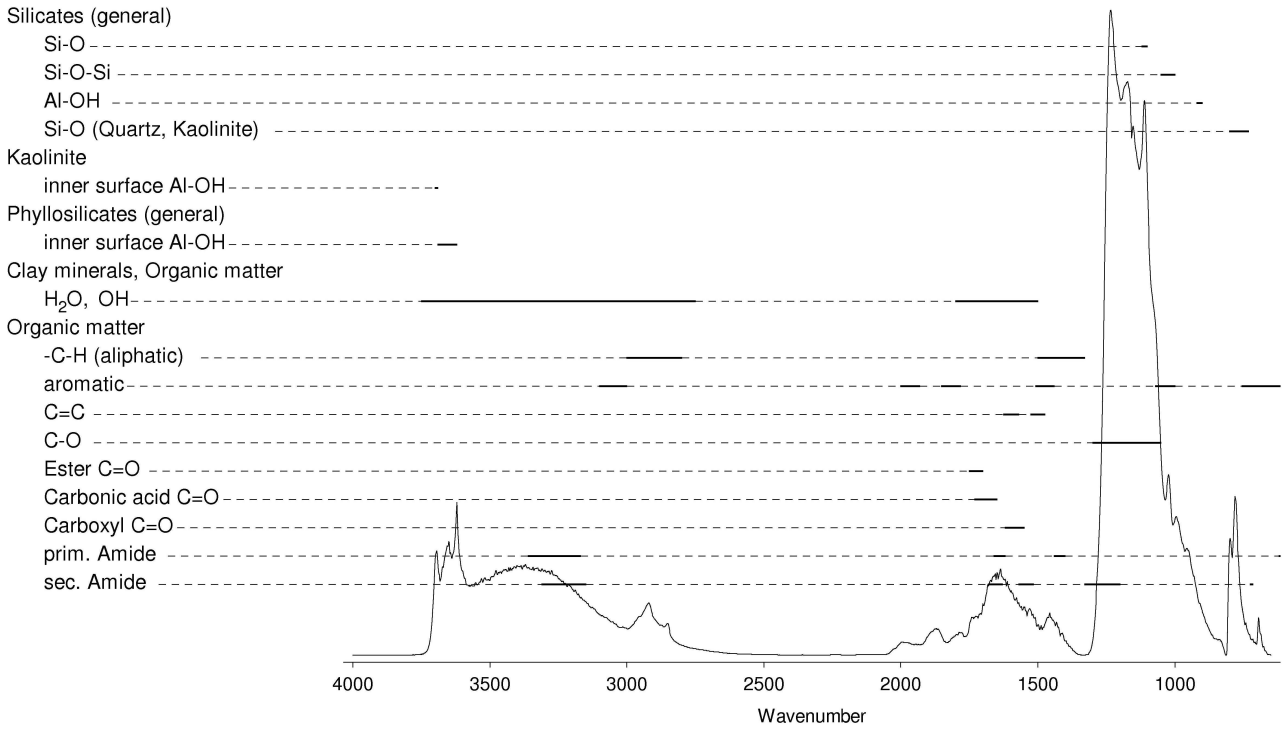
Silicates (general)
Si-O
Si-O-Si
Al-OH
Si-O (Quartz, Kaolinite)
Kaolinite
inner surface Al-OH
Phyllosilicates (general)
inner surface Al-OH
Clay minerals, Organic matter
H2O, OH
Organic matter
-C-H (aliphatic)
aromatic
C=C
C-O
Ester C=O
Carbonic acid C=O
Carboxyl C=O
prim. Amide
sec. Amide
4000
3500
3000
2500
2000
1500
1000
Wavenumber

Figure 6

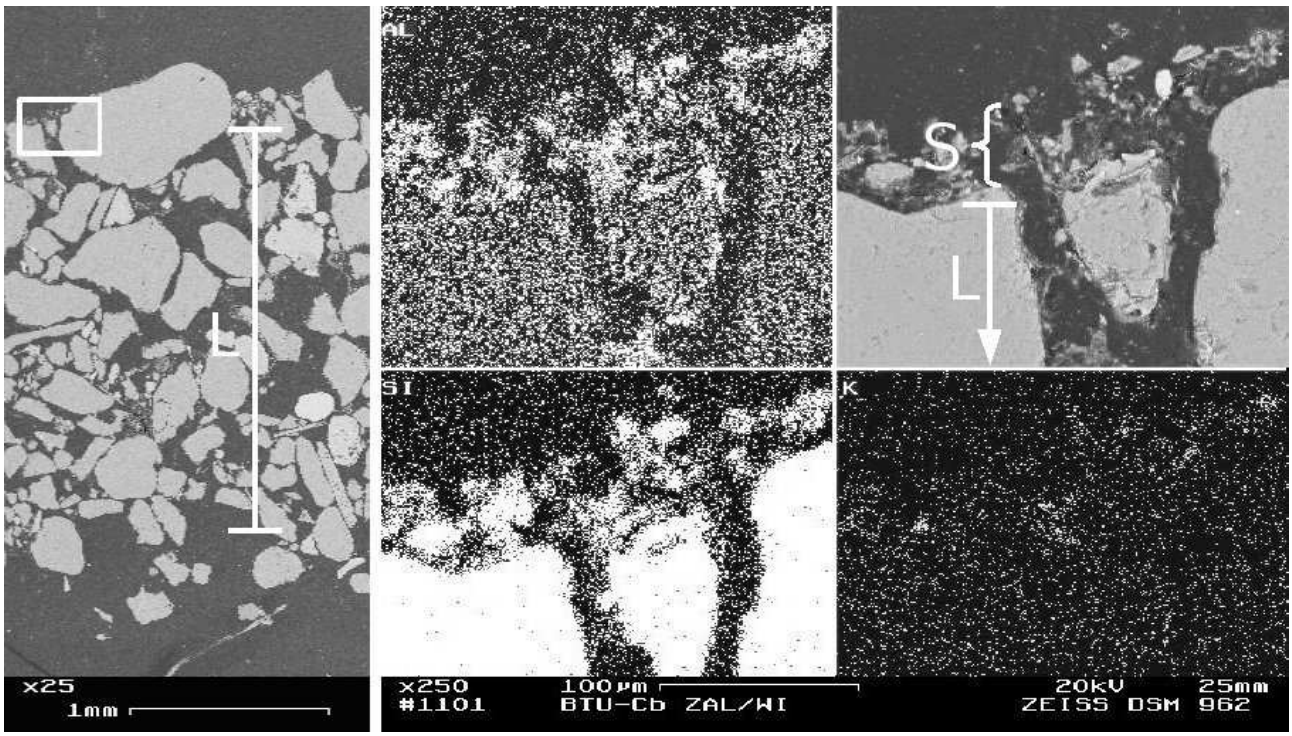
L
AL
S
L
SI
K
x25
1mm
x250
#1101
100µm
BTU-Cb ZAL/WI
20kV
25mm
ZEISS DSM 962

Figure 7

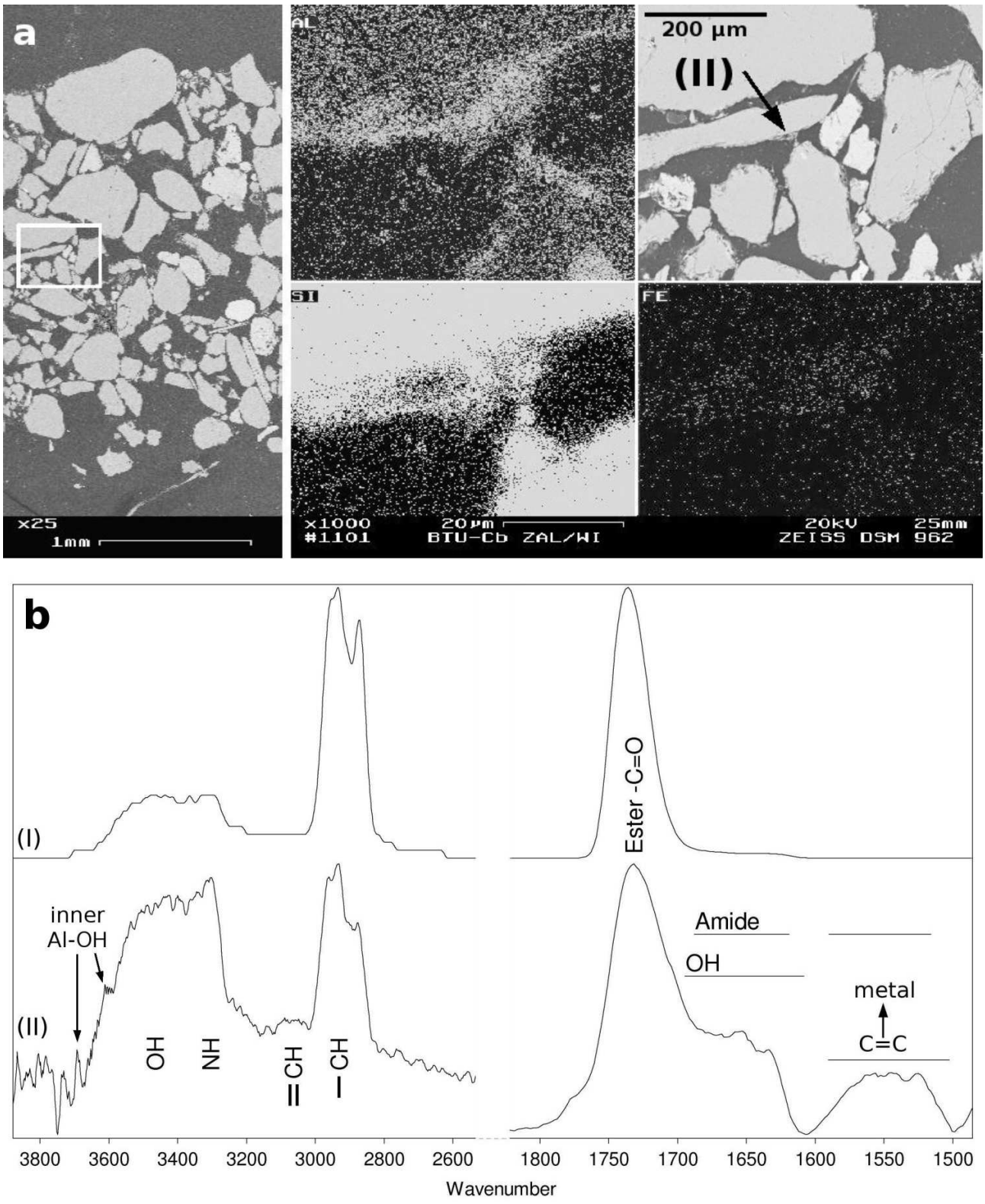
a
AL
200 µm
(II)
SI
FE
x25
1mm
x1000
#1101
20µm
BTU-Cb ZAL/WI
20kV
25mm
ZEISS DSM 962
b
(I)
Ester -C=O
inner
Al-OH
(II)
OH
NH
=CH
-CH
Amide
OH
metal
C=C
3800
3600
3400
3200
3000
2800
2600
1800
1750
1700
1650
1600
1550
1500
Wavenumber

Figure 8

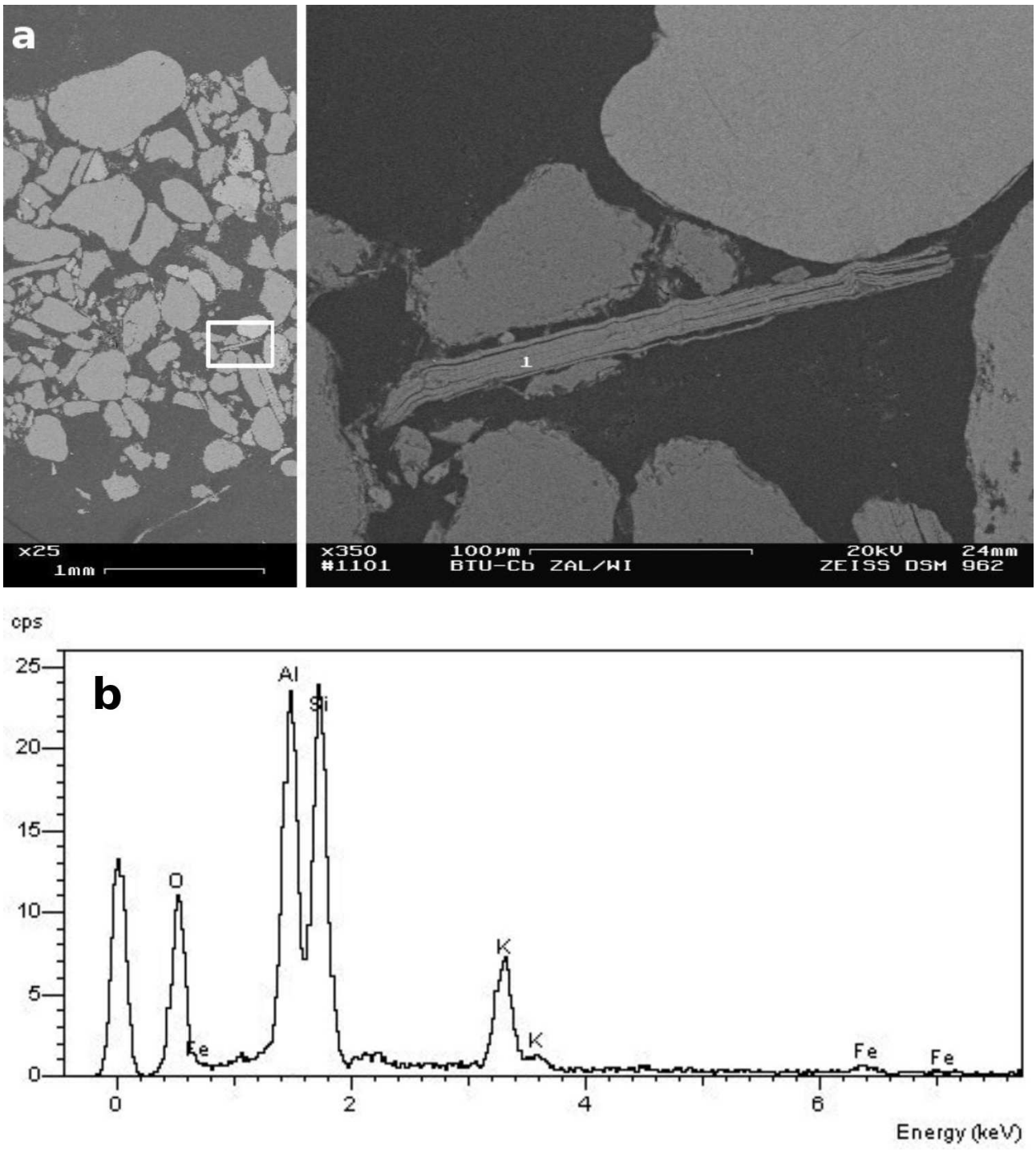
a
x25
1mm
x350
#1101
100µm
BTU-Cb ZAL/WI
20kV
ZEISS DSM 962
1
b
cps
25
20
15
10
5
0
O
Al
Si
Fe
K
K
Fe
Fe
0
2
4
6
Energy (keV)

Figure 9